HHS Public Access

Author manuscript

Dent Mater. Author manuscript; available in PMC 2020 January 01.

Published in final edited form as:

Dent Mater. 2019 January ; 35(1): 15–23. doi:10.1016/j.dental.2018.08.291.

Evaluating dental zirconia

Yu Zhang[1] and **Brian R Lawn**[2]

[1]Department of Biomaterials and Biomimetics, New York University College of Dentistry, New York, NY 10010, USA

[2]Material Measurement Laboratory, National Institute of Standards and Technology, Gaithersburg, MD 20899, USA

Abstract

Objectives.—To survey simple contact testing protocols for evaluating the mechanical integrity of zirconia dental ceramics. Specifically, to map vital material property variations and to quantify competing damage modes.

Methods and results.—Contact tests have been conducted on layer structures representative of zirconia crowns on dentin. Sharp-tip micro- and nano-indentations were used to explore the roles of weak interfaces and residual stresses in veneered zirconia, and to map property variations in graded structures. Tests with blunt sphere indenters on flat specimens were used to identify and quantify various critical damage modes in simulated occlusal loading in veneered and monolithic zirconia.

Significance.—Contact testing is a powerful tool for elucidating the fracture and deformation modes that control the lifetimes of zirconia dental ceramics. The advocated tests are simple, and provide a sound physical basis for analyzing damage resistance of anatomically-correct crowns and other complex dental prostheses.

Keywords

Indentation; zirconia; dental prostheses; fracture mode; fatigue; translucency

1. Introduction

The virtues of yttria stabilized tetragonal zirconia polycrystal (Y-TZP) as a dental ceramic are well documented [1-14]. There are many variants, but the mainstay is Y-TZP with 3 mol % yttria (3Y-TZP). While the strongest and toughest of the dental ceramics, Y-TZP is nevertheless not entirely immune to clinical failure over time [15-19]. This is an important consideration as new-generation zirconia materials with improved translucency (but potentially compromised strength and/or toughness) are developed [9,12,14,20-25].

Corresponding Author: Yu Zhang, Department of Biomaterials and Biomimetics, 433 First Avenue, Room 810, New York University College of Dentistry, New York, NY 10010, USA, yz21@nvu.edu, Tel.: +1-212-998-9637.

Elucidation of fracture and deformation mechanisms in these materials thereby holds the key to prolonged lifetimes of next-generation dental prostheses.

Prostheses such as crowns and bridges are essentially layer structures, seated and cemented onto a dentin base. They are subject to loading by occlusal contact and flexure, at high loads under onerous cyclic conditions in aqueous environments. Bite forces can exceed 1000 N [26] in well over 10^6 lifetime contact events [27,28]. It follows that testing protocols should at very least embody these basic elements of clinical geometry and stress state. Zirconia-based dental layer structures are of two main types: bilayer, in which a strong zirconia core is veneered with porcelain; single layer, where the entire prosthesis consists of zirconia in monolithic form. Traditional veneer/core structures are susceptible to failure from delamination and chipping of an esthetic but weak porcelain overlay, and to the presence of residual thermal stresses [29-37]. Monoliths avoid such issues but, at least in their basic 3Y-TZP form, lack translucency. The quest for ever more esthetic monolithic zirconias without compromising durability has become a driving force for materials development in the dental research community [12].

The question arises as to which laboratory testing methodology is best suited to reveal and quantify the various fracture modes that ultimately limit lifetimes of clinical zirconia. 'Standardized' mechanical tests that measure strength and toughness afford figures of merit for loosely ranking materials, but offer little physical insight into long-term performance or as to how critical configurational parameters may be optimized. They certainly have little provision to account for the variety of ways failure can occur in crown-like structures (Fig. 1a), especially those deformation processes that precede and drive some important fracture and wear modes [12]. A more pertinent yet straightforward approach is that of laboratory contact testing, using commercially available indenters to probe point-by-point property variations and to simulate occlusal and intaglio damage. Whereas the use of indentation as a numerical measure of material toughness has been queried [38], the methodology remains a uniquely powerful means of investigating a broad range of clinically relevant fracture and deformation modes in brittle materials [33,36,39,40].

In this study we apply indentation methods to model layer structures consisting of Y-TZP-based overlays cemented onto soft substrates, representative of zirconia prostheses on dentin. While basic tests are conducted on flat zirconia surfaces, precedent in the contact mechanics literature enables experimental and analytical extension to more complex, anatomically-correct geometries [41-44]. We demonstrate how tests with sharp-tip indenters can be used to map out property variations and to probe interface regions in multilayers. We also show how tests with sphere indenters can be employed to measure the extent to which fatigue and wear can significantly degrade strength properties of zirconia under adverse chewing conditions. Results surveyed from previous studies, along with new data, are presented as illustrative examples.

2. Materials and Testing

The bulk of the zirconia test material was obtained from commercial 3Y-TZP sources, fired and sintered according to manufacturers' specifications. Specimens were prepared in the

form of flat slabs with thickness ranging from 3 mm down to below 0.1 mm and with surface polish to 1 μm finish. All had a nominal strength near or above 1 GPa. Some Y-TZP specimens were tested as monoliths. Select specimens were prepared in-house with glass-infiltrated surfaces to produce graded structures [45]. Bilayer specimens of net thickness 1.5 mm were fabricated with either porcelain or a glass as veneer onto the zirconia core. Adjacent layers were joined by firing [46] or by cementation with a thin resin adhesive [47,48]. Thermal expansion mismatch conditions were noted in each case.

Select specimens were sectioned and side-polished. These were subjected to either micro-indentation using a Vickers diamond pyramid indenter, or to nano-indentation with a Berkovich diamond indenter in an automated test machine, to elucidate vital roles of any weak interfaces and strong residual stresses in bilayer structures or compositional concentration effects in graded structures.

To simulate occlusal damage modes representative of a zirconia-based crown on dentin, the slabs were first cemented onto a polycarbonate substrate as shown in the schematic configuration of Fig. 1b [48,49]. The top surface was then axially subjected to a single axial load/unload cycle with a spherical indenter of prescribed radius until damage was initiated in either the top or bottom surface of the cemented slab. The advantage of a flat specimen is that the damage modes may be observed, identified, analyzed and quantified with minimum geometrical complication. Use of a polycarbonate substrate also enables *in situ* undersurface viewing of any cracking at the intaglio interface, and serves to inhibit catastrophic propagation so that 'broken' specimens remain intact. Equivalent critical load data for a stiffer dentin substrate can be calculated using an explicit scaling relation for flexing plates on soft substrates (eqn. 1, below) [50]. If the slab itself is transparent or translucent the onset of top-surface damage can also be observed *in situ*; otherwise, critical loads could be determined in a microscope after unloading specimens with arrays of indents placed over a specified load range. As indicated above, complexities of anatomically-correct crown geometries and changes in substrate properties can be readily incorporated once the underlying damage modes are documented [42,48,51].

To quantify long-term flexure behavior, monolith zirconia specimens were tested in the same flat-surface configuration as Fig. 1b, but in repeat sphere axial loading up to 10^7 cycles [52]. In these tests the top surface was protected with a thin polymer film so that attention could be focused on potentially deleterious intaglio surface cracks. The specimen undersurfaces were prepared in three states before cementation to the polycarbonate base [52,53]: polished to 1 μm finish; sandblasted with 50 μm alumina grit; pre-indented with a sharp (Vickers) indenter at 10 N, representative of an errant microcontact impression or equivalent scratch of width ~ 20 μm.

Contact fatigue testing with spheres of radius 3.18 mm was conducted on zirconia bars 3 mm thick freely supported by a thick metal base plate, or discs 1.2 mm thick cemented onto a composite support base. (It has been demonstrated that the modulus or hardness of the sphere is not a critical factor, as long as these quantities remain equal or greater to those of the specimen material [54].) Repeat indentation tests were made at prescribed maximum loads up to 1000 N over 10^6 cycles, either axially on a crosshead testing machine [55] or in

sliding contact in a mouth-motion machine [56]. Optical microscopy reveals marked surface damage in these tests, akin to severe wear facets. The indented specimens were then broken in fast 4-point flexure (bars) or piston-on-3-ball biaxial flexure (discs) in a dry environment, with damage sites centered on the tensile side, to quantify 'inert' strength. Those specimens suffering strength degradation failed from the indentation sites.

3. Results

3.1 Exploratory mapping

The utility of indentation techniques as a means of mapping spatial variations in material properties is demonstrated in Fig. 2. In the two examples shown, software in an automated nanoindenter test machine is programmed to place an array of Berkovich nanoindentations across specimen sections. The software routinely deconvolutes elastic modulus E (and hardness H) from the load-displacement functions at each contact site [57]. Figure 2a shows elastic modulus profiles across tooth enamel sections in the great apes (human, orangutan, chimpanzee, gorilla) [58]. The data confirm that enamel is stiffer (and harder) near the tooth outer surface [59]. Comparative variations are evident in indentation toughness measurements [60]. Interestingly, the data in Fig. 2a show little difference between the various ape species, consistent with (if not definitive evidence for) a common ancestry [61].

Figure 2b shows an analogous E profile in an in-house glass-infiltrated 3Y-TZP [62], The value ~ 70 GPa at the outer surface is close to that of tooth enamel or porcelain, with a smooth transition to the value for bulk zirconia over an infiltration depth −150 μm. The absence of an abrupt internal interface avoids a potential source of weakness in the structure. Further benefits of infiltration are enhanced shade selection at the cameo surface [25] and greater bond strength at the intaglio surface [63]. The advantages of nanoindentation property mapping of this kind should become even more apparent as new biomimetic zirconias and other inhomogeneous dental ceramics are developed.

Microindentation with a Vickers diamond pyramid is a valuable site-specific tool for probing properties of interfaces in dental bilayer structures. Figure 3 shows examples for a 3Y-TZP zirconia core veneered with (a) dental porcelain and (b) borosilicate glass [46]. For the porcelain-veneered structures in Fig. 3a, thermal expansion coefficients were matched ($< 0.5\times10^{-6}\ ^{\circ}C^{-1}$) so as to generate minimal residual stresses. Vickers indentations with well-defined corner cracks (10 N in porcelain, 40 N in Y-TZP) are placed close to the interface. The lead crack emanating from the porcelain indent is seen to arrest at the interface. Indents placed even closer to the interface lead to delamination. In no case did a crack from a porcelain indent traverse into the tougher zirconia core. The behavior is quite different for cracks emanating from indents in the zirconia. In those cases the cracks penetrate readily into the weaker porcelain without any delamination. The methodology provides a clear visual picture of the role of a weak interface for cracks originating in either the veneer or core. It also has provision for rigorous fracture mechanics analysis, with due allowance for important effects of mismatch in elastic modulus [64], enabling quantification of the interface toughness [46,65].

Whereas in Fig. 3a care was taken to choose a veneer with small thermal expansion mismatch, in Fig. 3b a borosilicate glass veneer was selected to give a deliberately large expansion differential ($< 5\times10^{-6}$ °C^{-1}) [46]. Mismatch of this order induces lateral tensile stresses in excess of 150 MPa into the zirconia core (compression in the porcelain veneer). A Vickers indentation in the 3Y-TZP core has penetrated into the veneer as before but, exacerbated by slow crack growth, has traversed the entire zirconia core. Note also the deflection of adjacent corner cracks nearly parallel to the interface. The influence of excessive thermal expansion mismatch is visually palpable, reinforcing the need to pay close attention to property matching in bilayer structures.

3.2 Simulated occlusal contact

Results of contact tests with a single-cycle sphere axial contact on flat monolith zirconia and veneered zirconia slabs bonded to soft substrates are shown in Fig. 4 [66,67]. Critical loads to initiate the various damage modes (Fig. 1b) in the Y-TZP/substrate specimens are plotted as a function of zirconia thickness d in Fig. 4a, in the veneer/Y-TZP/substrate specimens as a function of zirconia core thickness d_2 in Fig. 4b but with fixed *net* veneer+core thickness $d = d_1 + d_2 = 1.5$ mm. Data points are loads P_R at which subsurface radial cracks are observed to initiate from the intaglio zirconia surface. The solid curves in Fig. 4a are theoretical predictions from the stress solution for a flexing zirconia plate on soft substrate [67]

$$P_R = BSd^2/\log(E_z/Es) \quad (1)$$

where E_z and E_s are elastic moduli of zirconia and substrate respectively, S is the strength of zirconia, d is the net layer thickness and B is a coefficient. While the tests were conducted on polycarbonate substrates for experimental expediency, the P_R data in Fig. 4 have been adjusted to match dentin substrates using appropriate modulus ratios in eqn. 1. For the trilayer veneer/Y-TZP/substrate structure in Fig. 4b, an extra multiplicative factor to allow for veneer/core modulus and thickness ratios has to be incorporated into the right-hand side of eqn. 1 [67]. It is noteworthy in this latter case that the zirconia core, although much stronger than the overlaying veneer, is still subject to intaglio radial cracking, owing to the concentration of tensile stress at the lower surface of the flexing bilayer plate beneath the contact site [67]. It is also noteworthy that P_R is not sensitive to the actual core thickness in Fig. 4b, provided the *net* thickness d remains fixed.

Also included as dashed lines in the plot for the Y-TZP/substrate bilayer in Fig. 4a are predictions of critical loads P_Y and P_C to produce top-surface yield (quasiplastic) deformation and peripheral cone cracking in axial contact [48,68,69]

$$P_C = A(T^2/E)r \quad (2a)$$

$$P_Y = DH(H/E)^2r^2 \quad (2b)$$

where T and H are toughenss and hardness of zirconia and A and D are coefficients, here plotted for a nominal sphere radius $r = 5$ mm. Note that P_R in eqn. 1 depends on d but not r, whereas P_C and P_Y in eqn. 2 depend on r but not d. Thus the dashed P_C and P_Y lines in Fig. 4a will move up and down the plot as r varies, but the solid P_R line will be unchanged. Conversely, points will progress down the P_R curve as d diminishes, but P_C and P_Y will remain unchanged. Thus while yield and even cone cracking are likely to initiate first in thicker zirconia specimens, subsurface radial cracking will rapidly become the dominant threat as thickness diminishes much below 1 mm.

The single-contact data in Fig. 4 are useful for identifying conditions under which each potential damage mode is likely to initiate. It is important to ask how these damage modes will evolve in the long term, after repeat occlusal cycles. Critical contact loads to generate intaglio radial cracks in multi-contact tests on monolithic Y-TZP are shown in Fig. 5 for various subsurface states [52] (again using eqn. 1 to adjust experimental data to match dentin substrates [53]). The straight lines for polished and sandblasted surfaces are predictions in accordance with strength degradation from chemically-assisted slow crack growth acting on critical flaws. Load-bearing capacity in these two instances is degraded by more than a factor of 2 over some million or more cycles, i.e. typical of chewing frequencies over 5 years or so [27,28]. The sandblasted surfaces are some 30% weaker than polished surfaces over the cyclic range, demonstrating the potentially deleterious effects of undersurface roughening prior to fitting of a crown. The degradation is even stronger for zirconia surfaces with a controlled light-load indentation flaw, by up to some 80% [70,71]. Moreover, the falloff over the cyclic range is faster than predicted from slow crack growth alone, indicative of some additional, mechanical fatigue mechanism within the quasiplastic contact zone [52]. Such data suggest care to avoid deep surface scratches from errant sharp particles [72] or coarse diamond drill burs during prosthesis preparation or finishing [73].

Figure 6 plots remaining strength S of monolithic zirconia after prior cyclic contact at the occlusal surface from a sphere of radius $r = 3.18$ mm, for (a) axial and (b) sliding loading. The degradation is particularly marked for sliding tests in Fig. 6b: note the enhanced dropoff in strength after a relatively small number of cycles, and at a much lower contact load than that for axial loading in Fig. 6a. *Post mortem* examination of the contact sites in zirconia and other ceramics reveals progressive buildup of surface attrition with continued cycling [55]. Ultimately, coalescence of microcracks within the quasiplastic zone into macroscopic cone (or other) cracks, exacerbated by enhanced tensile stresses in sliding mode [74], accounts for the abrupt strength dropoffs. The degradation is determined by number of cycles rather than total contact time, meaning that the degradation is predominantly mechanical in nature [75]. These results add substance to our contention that standard strength tests on pristine material surfaces, even incorporating slow crack growth into the flaw mechanics, are an inadequate guide to long-term performance.

4. Discussion

Dental zirconia ceramics are relatively strong and tough, but are subject to property variations and degradation of load-bearing capacity over time. There is a place for clinically relevant testing procedures that can map out such variations and that can identify and

elucidate competing damage modes (Fig. 1a). Indentation testing is a simple but uniquely powerful methodology that meets this need. Judicially placed micro-and nano-indentations in specimen sections can clarify the roles of internal interfaces and property gradients: in bilayer structures, residual stresses from thermal expansion mismatch and interface toughnesses can be evaluated; in graded structures, mechanical properties can be traced out across a specimen section. In many instances indentation mapping is the only practical way to explore and quantify such elements. It promises to become ever more useful as more biomimetic dental materials with elaborate microstructures and layer configurations are developed.

Testing of flat layer zirconia layers on a soft support with blunt, spherical indenters (Fig. 1b) takes us closer to actual occlusal loading conditions than do 'standardized' strength and toughness test protocols. Chewing involves complex mouth motion [27,76], but is essentially a contact process. Contact testing affords visual and quantitative evaluation of the susceptibility of dental zirconias to fundamental mechanisms of fracture and deformation. It contains provision for cyclic loading, axial or sliding, in aqueous environments. It enables damage modes to be identified and analyzed in terms of explicit critical load relations (eqns. 1 and 2). The use of flat specimens is not restrictive, since the geometrical complexities of anatomically-correct prostheses can readily be analyzed in conjunction with extended finite element methods [43,51,77,78].

Figure 1 depicts two basic classes of damage in dentin-supported zirconia layer structures:

(i) *Intaglio radial cracks*. These cracks usually initiate from the intaglio surface immediately below the contact zone. They are subject to high tensile stress states in plate flexure, especially dominant in thinner layers, so are more likely to grow into longitudinal or even splitting cracks that traverse the entire height of the prosthesis [43,51,79]. Initiation of such cracks is conveniently visible in simple tests on transparent test substrates (Fig. 1b) [66]. The presence of a thin compliant cementation layer between ceramic overlay and substrate can substantially lower the critical load for radial crack initiation [80]. In certain cases, e.g. loading with a soft contact, radial cracks may also generate at the margins in anatomically-correct crown structures [81]. The roles of surface states associated with undersurface preparation prior to fitting, e.g. sandblasting, grinding, scratching etc. can be readily quantified (Fig. 5).

(ii) *Occlusal surface damage modes*. It can be argued that occlusal damage modes should be less deleterious, since typical occlusal contacts are arguably blunter than those used in the current tests, with consequent diminution of contact pressures below those needed to initiate quasiplastic deformation [82]. Moreover, measurements of actual occlusal contact areas using pressure-sensitive film techniques indicate that while bite forces can indeed exceed 1000 N, these forces are distributed along the entire dentition in normal clenching, with further diminution of local contact pressures in an individual tooth or crown prosthesis [26]. Also, flexural stresses at the top surface are predominantly compressive during normal chewing activity, so incipient crack initiation may be subdued. However, local high pressures sufficient to induce top-surface yield in a crown structure could occur in biting on a hard object with high curvature (e.g. fruit pit, ice cube, bone fragment, eating utensil). Any

sliding component in the contact stress field would further enhance the onset of top-surface damage [83]. As noted in Fig. 6, damage of this kind is cumulative and far from benign. Any cracks that emerge from the contact zone and grow into the lower reaches of a zirconia layer, especially under cyclic fatigue conditions, will be subject to flexural tension [84,85], Such cracks have been observed to traverse the entire thickness of a supported ceramic plate in ball-on-flat tests [53]. In any event, the strength data in Fig. 6 usefully serve to quantify how rapidly, and to what extent, Y-TZP degrades under extreme contact fatigue conditions. More extensive contact testing also reveals subsidiary damage modes, such as inner cone cracks from hydraulic pumping, median cracks from coalescence of microcracks within a quasiplastic zone, chipping from near-edge contacts, delamination, etc. (Fig. 1a) [44,53], Shallow material removal processes at wear facets from multiple abrasive microcontacts at lower contact pressures, superficially akin to quasiplasticity damage but surface-localized, can also act as sources of failure.

New zirconia ceramics for dental restorations are continually under development, with a goal of maintaining mechanical integrity while improving translucency [12,25,44], The trend is toward monoliths, for greater longevity and avoidance of interfacial and residual stress issues. Compositional variants—graded structures, biomimetic structures, nanostructures—are being explored. An understanding of basic damage processes is a vital complement to the continued development of more esthetic yet durable zirconias.

Acknowledgements

The authors thank Marcia Borba and Tomoyuki Okamoto for providing the strength degradation data in Fig. 6b. Funding was provided by the U.S. National Institute of Dental and Craniofacial Research (Grant Nos. R01DE017925, R01DE026279 and R01DE026772) and National Science Foundation (Grant No. CMMI-0758530). Information of product names and suppliers in this paper is not to imply endorsement by NIST.

References

1. Denry I, Kelly JR. State of the art of zirconia for dental applications. Dent Mater 2008; 24:299–307. [PubMed: 17659331]
2. Rekow ED, Silva NRFA, Coehlo PG, Zhang Y, Guess P, Thompson VP. Performance of dental ceramics: Challenges for improvements. J Dent Res 2011; 90:937–952. [PubMed: 21224408]
3. Kelly JR, Benetti P. Ceramic materials in dentistry: Historical evolution and current practice. Australian Dental Journal 2011; Suppl 1:84–96. [PubMed: 21564119]
4. Almazdi AA, Khajah KM, Monaco EA, Kim H. Applying microwave technology to sintering dental zirconia. J Prosthet Dent 2012; 108:304–309. [PubMed: 23107238]
5. Stober T, Bermejo JL, Rammelsberg P, Schmitter M. Enamel wear caused by monolithic zirconia crowns after 6 months of clinical use. J Oral Rehab 2014; 41:314–322.
6. Mundhe K, Jain V, Pruthi G, Shah N. Clinical study to evaluate the wear of natural enamel antagonist to zirconia and metal ceramic crowns. J Prosthet Dent 2015; 114:358–363. [PubMed: 25985742]
7. Zhang F, Inokoshi M, Batuk M, Hadermann J, Naert I, VanMeerbeek B, Vleugels J. Strength, toughness and aging stability of highly-translucent Y-TZP ceramics for dental restorations. Dent Mater 2016; 32:e327–337. [PubMed: 27697332]
8. Pieralli S, Kohal RJ, Jung RE, Vach K, Spies BC. Clinical outcomes of zirconia dental implants: A systematic review. J Dent Res 2017; 96:38–46. [PubMed: 27625355]
9. Sulaiman TA, Abdulmajeed AA, Shahramian K, Lassila L. Effect of different treatments on the flexural strength of fully versus partially stabilized monolithic zirconia. J Prosthet Dent 2017; 118:216–220. [PubMed: 28159339]

10. Kaizer MR, Guess PC, Dos Santos MBF, Cava SS, Zhang Y. Speed sintering translucent zirconia for chairside one-visit dental restorations: Optical, mechanical, and wear characteristics Ceramics International 2017; in press:
11. Bömicke W, Rammelsberg P, Stober T, Schmitter M. Short-term prospective clinical evaluation of monolithic and partially veneered zirconia single crowns. Journal of Esthetic and Restorative Dentistry 2017; 29:22–30. [PubMed: 27679981]
12. Zhang Y, Lawn BR. Novel zirconia materials in dentistry. J Dent Res 2018; 97:140–147. [PubMed: 29035694]
13. Esquivel-Upshaw JF, Kim MJ, Hsu SM, Abdulhameed N, Jenkins R, Neal D, Ren F. Randomized clinical study of wear of enamel antagonists against polished monolithic zirconia crowns. J Dentistry 2018; 68:19–27.
14. Pereira GKR, Guilardi LF, Dapieve KS, Kleverlaan CJ, Rippe MP, Valandro LF. Mechanical reliability, fatigue strength and survival analysis of new polycrystalline translucent zirconia ceramics for monolithic restorations. J Mech Behav Biomed Mater 2018; 85:57–65. [PubMed: 29857261]
15. Sax C, Hämmerle CH, Sailer I. 10-year clinical outcomes of fixed dental prostheses with zirconia frameworks. Int J Comput Dent 2011; 14:183–201. [PubMed: 22141229]
16. Salido MP, Martinez-Rus F, del Rio F, Pradies G, Ozcan M, Suarez MJ. Prospective clinical study of zirconia-based posterior four-unit fixed dental prostheses: Four-year follow-up. Int J Prosthodont 2012; 25:403–409. [PubMed: 22720293]
17. Schmitter M, Mussoter K, Rammelsberg P, Gabbert O, Ohlmann B. Clinical performance of long-span zirconia frameworks for fixed dental prostheses: 5-year results. J Oral Rehab 2012; 39:552–557.
18. Sulaiman TA, Abdulmajeed AA, Donavan TR, Cooper LF, Walter R. Fracture rate of monolithic zirconia restorations up to 5 years: A dental laboratory study. J Prosthet Dent 2016; 116:436–439. [PubMed: 27178771]
19. Abdulmajeed AA, Donovan TE, Cooper LF, Walter R, Sulaiman TA. Fracture of layered zirconia restorations at 5 years: A dental laboratory survey. J Prosthet Dent 2017; 118:353–356. [PubMed: 28222877]
20. McLaren EA, Lawson N, Choi J, Kang J, Trujillo C. New high-translucent cubic-phase-containing zirconia: Clinical and laboratory considerations and the effect of air abrasion on strength. Compend Cont Educat Dentistry 2017; 38:e13–16.
21. Inokoshi M, Shimizu H, Nozaki K, Takagaki T, Yoshihara K, Nagaoka N, Zhang F, Vleugels J, Van Meerbeek B, Minakuchi S. Crystallographic and morphological analysis of sandblasted highly translucent dental zirconia. Dent Mater 2018; 34:508–518. [PubMed: 29325861]
22. Wille S, Zumstrull P, Kaidas V, Jessen LK, Kern M. Low temperature degradation of single layers of multilayered zirconia in comparison to conventional unshaded zirconia: Phase transformation and flexural strength. J Mech Behav Biomed Mater 2018; 77:171–175. [PubMed: 28918009]
23. Kwon SJ, Lawson NC, McLaren EE, Nejat AH, Burgess JO. Comparison of the mechanical properties of translucent zirconia and lithium disilicate. J Prosthet Dent 2018; 120:132–137. [PubMed: 29310875]
24. Camposilvan E, Leone R, Gremillard L, Sorrentino R, Zarone F, Ferrari M, Chevalier J. Aging resistance, mechanical properties and translucency of different yttria-stabilized zirconia ceramics for monolithic dental crown applications. Dent Mater 2018; 34:879–890. [PubMed: 29598882]
25. Mao L, Kaizer MR, Zhao M, Guo B, Song YF, Zhang Y. Graded ultra-translucent zirconia (5Y-PSZ) for strength and functionalities. J Dent Res 2018; in press:
26. Hidaka O, Iwasaki M, Saito M, Moromoto T. Influence of clenching intensity on bite force balance, occlusal contact area, and average bite pressure. J Dent Res 1999; 78:1336–1344. [PubMed: 10403461]
27. DeLong R, Douglas WH. Development of an artificial oral environment for the testing of dental restoratives: Bi-axial force and movement control. J Dent Res 1983; 62:32–36. [PubMed: 6571851]
28. Krejci I, Lutz F. In-vitro test results of the evaluation of dental restoration systems: Correlation with in-vivo results. Schweiz Monatsschr Zahnmed 1990; 100:1445–1449. [PubMed: 2277977]

29. Swain MV. Unstable cracking (chipping) of veneering porcelain on all-ceramic dental crowns and fixed partial dentures. Acta Biomater 2009; 5:1668–1677. [PubMed: 19201268]
30. Tholey MJ, Swain MV, Thiel N. Thermal gradients and residual stresses in veneered Y-TZP frameworks. Dent Mater 2011; 27:1102–1110. [PubMed: 21907400]
31. Mainjot AJ, Shajer GS, Vanheusden AJ, Sadoun MJ. Residual stress measurement in veneering ceramic by hole-drilling. Dent Mater 2011; 27:439–444. [PubMed: 21232786]
32. Mainjot AJ, Shajer GS, Vanheusden AJ, Sadoun MJ. Influence of cooling rate on residual stress profile in veneering ceramic: Measurement by hole-drilling. Dent Mater 2011; 27:906–914. [PubMed: 21676454]
33. Baldassarri M, Stappert CF, Wolff MS, Thompson VP, Zhang Y. Residual stresses in porcelain-veneered zirconia prostheses. Dent Mater 2012; 28:873–879. [PubMed: 22578663]
34. Belli R, Monteiro S, Jr., Baratieri LN, Katte H, Petschelt A, Lohbauer U. A photoelastic assessment of residual stresses in zirconia-veneer crowns. J Dent Res 2012; 91:316–320. [PubMed: 22262632]
35. Benetti P, Kelly JR, Della Bona A. Analysis of thermal distributions in veneered zirconia and metal restorations during firing. Dent Mater 2013; 28:1166–1172.
36. Wendler M, Belli R, Petschelt A, Lohbauer U. Characterization of residual stresses in zirconia veneered bilayers assessed via sharp and blunt indentation. Dent Mater 2015; 31:948–957. [PubMed: 26037789]
37. Kim J, Dhital S, Zhivago P, Kaizer MR, Zhang Y. Viscoelastic finite element analysis of residual stresses in porcelain-veneered zirconia dental crowns. J Mech Behav Biomed Mater 2018; 82:202–209. [PubMed: 29621687]
38. Cesar PF, Bona AD, Scherrer SS, Tholey M, vanNoort R, Vichi A, Kelly R, Lohbauer U. Adm guidance—ceramics: Fracture toughness testing and method selection. Dent Mater 2017; 33:575–584. [PubMed: 28392020]
39. Kelly JR, Benetti P, Rungruanganunt P, Bona AD. The slippery slope: Critical perspectives on in vitro research methodologies. Dent Mater 2012; 28:41–51. [PubMed: 22192250]
40. Marshall DB, Cook RF, Padture NP, Oyen ML, Pajares A, Bradby JE, Reimanis IE, Tandon R, Page TF, Pharr GM, Lawn BR. The compelling case for indentation as a functional exploratory and characterization tool. J Amer Ceram Soc 2015; 98:2671–2680.
41. Qasim T, Bush MB, Hu X, Lawn BR. Contact damage in brittle coating layers: Influence of surface curvature. Journal of Biomedical Materials Research 2005; 73B: 179–185.
42. Rekow ED, Zhang G, Thompson V, Kim JW, Coehlo P, Zhang Y. Effects of geometry on fracture initiation and propagation in all-ceramic crowns. Journal of Biomedical Materials Research 2009; B88:436–446.
43. Barani A, Chai H, Lawn BR, Bush MB. Mechanics analysis of molar tooth splitting. Acta Biomater 2015; 15:237–243. [PubMed: 25584989]
44. Zhang Y, Mai Z, Barani A, Bush M, Lawn B. Fracture-resistant monolithic dental crowns. Dent Mater 2016; 32:442–449. [PubMed: 26792623]
45. Zhang Y, Chai H, Lawn BR. Graded structures for all-ceramic restorations. J Dent Res 2010; 89:417–421. [PubMed: 20200413]
46. Kim J-W, Bhowmick S, Hermann I, Lawn BR. Transverse fracture of brittle layers: Relevance to failure of all-ceramic dental crowns. Journal of Biomedical Materials Research 2006; 79B:58–65.
47. Miranda P, Pajares A, Guiberteau F, Cumbrera FL, Lawn BR. Contact fracture of brittle bilayer coatings on soft substrates. J Mater Res 2001; 16:115–126.
48. Lawn BR, Deng Y, Miranda P, Pajares A, Chai H, Kim DK. Overview: Damage in brittle layer structures from concentrated loads. J Mater Res 2002; 17:3019–3036.
49. Lawn BR, Deng Y, Thompson VP. Use of contact testing in the characterization and design of all-ceramic crown-like layer structures: A review. J Prosthet Dent 2001; 86:495–510. [PubMed: 11725278]
50. Lee KS, Rhee Y-W, Blackburn DH, Lawn BR, Chai H. Cracking of brittle coatings adhesively bonded to substrates of unlike modulus. J Mater Res 2000; 15:1653–1656.

51. Barani A, Keown AJ, Bush MB, Lee JJ-W, Chai H, Lawn BR. Mechanics of longitudinal cracks in tooth enamel. Acta Biomater 2011; 7:2285–2292. [PubMed: 21296195]
52. Zhang Y, Lawn BR. Fatigue sensitivity of Y-TZP to microscale sharp-contact flaws. Journal of Biomedical Materials Research 2005; 72B:388–392.
53. Zhang Y, Sailer I, Lawn BR. Fatigue of dental ceramics. J Dentistry 2013; 41:1135–1147.
54. Bhowmick S, Mélendez-Martinez JJ, Herman I, Zhang Y, Lawn BR. Role of indenter material and size in veneer failure of brittle layer structures. Journal of Biomedical Materials Research 2007; 82B:253–259.
55. Jung Y-G, Peterson IM, Kim DK, Lawn BR. Lifetime-limiting strength degradation from contact fatigue in dental ceramics. J Dent Res 2000; 79:722–731. [PubMed: 10728973]
56. Kim JH, Kim JW, Myoung SW, Pines M, Zhang Y. Damage maps for layered ceramics under simulated mastication. J Dent Res 2008; 87:671–675. [PubMed: 18573989]
57. Oliver WC, Pharr GM. An improved technique for determining hardness and elastic-modulus using load and displacement sensing indentation experiments. J Mater Res 1992; 7:1564–1583.
58. Lee JJ-W, Morris D, Constantino PJ, Smith TM, Lawn BR. Properties of tooth enamel in great apes. Acta Biomater 2010; 6:4560–4565. [PubMed: 20656077]
59. Cuy JL, Mann AB, Livi KJ, Teaford MF, Weihs TP. Nanoindentation mapping of the mechanical properties of human molar tooth enamel. Arch Oral Biol 2002; 7:281–291.
60. Imbeni V, Kruzic JJ, Marshall GW, Marshall SJ, Ritchie RO. The dentin–enamel junction and the fracture of human teeth. Nature Mater 2005; 4:229–232. [PubMed: 15711554]
61. Constantino PJ, Lee JJ-W, Grbig Y, Hartstone-Rose A, Talebi M, Lawn BR, Lucas PW. The role of tooth enamel mechanical properties in primate dietary adaptation. Amer J Phys Anthropol 2012; 148:171–177. [PubMed: 22610893]
62. Zhang Y, Kim JW. Graded structures for damage resistant and aesthetic all-ceramic restorations. Dent Mater 2009; 25:781–790. [PubMed: 19187955]
63. Chai H, Kaizer M, Chughtai A, Tong H, Tanaka C, Zhang Y. On the interfacial fracture resistance of resin-bonded zirconia and glass-infiltrated graded zirconia. Dent Mater 2015; 31:1304–1311. [PubMed: 26365987]
64. He M-Y, Hutchinson JW. Crack deflection at an interface between dissimilar elastic materials. Int J Solids Struct 1989; 25:1053–1067.
65. Becher PF, Sun EY, Hseuh CH, Alexander KB, Waters SL, Westmoreland CG. Debonding of interfaces between beta-silicon nitride whiskers and Si-Al-Y oxynitride glasses. Acta Mater 1996; 44:3881–3893.
66. Deng Y, Lawn BR, Lloyd IK. Characterization of damage modes in dental ceramic bilayer structures. Journal of Biomedical Materials Research 2002; 63B: 137–145.
67. Deng Y, Miranda P, Pajares A, Guiberteau F, Lawn BR. Fracture of ceramic/ceramic/polymer trilayers for biomechanical applications. Journal of Biomedical Materials Research 2003; 67A: 828–833.
68. Rhee Y-W, Kim H-W, Deng Y, Lawn BR. Brittle fracture versus quasiplasticity in ceramics: A simple predictive index. J Amer Ceram Soc 2001; 84:561–565.
69. Rhee Y-W, Kim H-W, Deng Y, Lawn BR. Contact-induced damage in ceramic coatings on compliant substrates: Fracture mechanics and design. J Amer Ceram Soc 2001; 84:1066–1072.
70. Cook RF, Braun LM, Cannon WR. Trapped cracks at indentations: I. Experiments on yttria-tetragonal zirconia polycrystals. J Mater Sci 1994; 29:2133–2142.
71. Cook RF, Braun LM. Trapped cracks at indentations: Ii. Fracture mechanics model. J Mater Sci 1994; 29:2192–2204.
72. Borrero-Lopez O, Pajares A, Constantino P, Lawn BR. Mechanics of microwear traces in tooth enamel. Acta Biomater 2015; 14:146–153. [PubMed: 25484336]
73. Kosmac T, Oblak C, Jevnikar P, Funduk N, Marion L. The effect of surface grinding and sandblasting on flexural strength and reliability of Y-TZP zirconia ceramic. Dent Mater 1999; 15:426–433. [PubMed: 10863444]
74. Lawn BR. Partial cone crack formation in a brittle material loaded with a sliding indenter. Proc Roy Soc Lond 1967; A299:307–316.

75. Kim DK, Jung Y-G, Peterson IM, Lawn BR. Cyclic fatigue of intrinsically brittle ceramics in contact with spheres. Acta Mater 1999; 47:4711–4725.

76. Ulhaas L, Kullmer O, Schrenk F, Henke W. A new 3-d approach to determine functional morphology of cercopithecoid molars. Anatomische Gesellschaft 2004; 186:487–493.

77. Rudas M, Qasim T, Bush MB, Lawn BR. Failure of curved brittle layer systems from radial cracking in concentrated loading. J Mater Res 2005; 20:2812–2819.

78. Barani A, Bush MB, Lawn BR. Effect of property gradients on enamel fracture in human enamel. J Mech Behav Biomed Mat 2012; 15:121–130.

79. Campos RE, Soares PV, Versluis A, Júnior OBdO. Crown fracture: Failure load, stress distribution, and fractographic analysis. J Prosthet Dent 2015; 114:447–455. [PubMed: 26001492]

80. Kim JH, Miranda P, Kim DK, Lawn BR. Effect of an adhesive interlayer on the fracture of a brittle coating on a supporting substrate. J Mater Res 2003; 18:222–227.

81. Qasim T, Ford C, Bush MB, Hu X, Malament KA, Lawn BR. Margin failures in brittle dome structures: Relevance to failure of dental crowns Journal of Biomedical Materials Research 2007; 80B:78–85.

82. Kelly JR, Rungruanganunt P, Hunter B, Vallati F. Development of a clinically validated bulk failure test for ceramic crowns. J Prosthet Dent 2010; 104:228–238. [PubMed: 20875527]

83. Ren L, Zhang Y. Sliding contact fracture of dental ceramics: Principles and validation. Acta Biomater 2014; 10:3243–3253. [PubMed: 24632538]

84. Bhowmick S, Zhang Y, Lawn BR. Competing fracture modes in brittle materials subject to concentrated cyclic loading in liquid environments: Bilayer structures. J Mater Res 2005; 20:2792–2800.

85. Zhang Y, Song J-K, Lawn BR. Deep penetrating conical cracks in brittle layers from hydraulic cyclic contact. Journal of Biomedical Materials Research 2005; 73B:186–193.

86. Deng Y, Lawn BR, Lloyd IK. Damage characterization of dental materials in ceramic-based crown-like layer structures. Key Eng Mat 2001; 224–26:453–457.

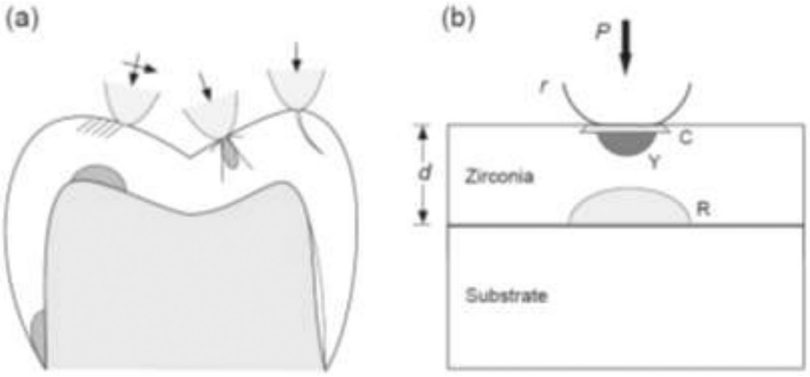

1.

Failure modes in ceramic layers on soft substrates. (a) Schematic of crown on dentin, showing fracture and deformation modes at occlusal and cementation surfaces from axial, sliding and edge contacts [12]. (b) Basic experimental setup, indicating damage modes from sphere indenter of radius r at axial load P on flat zirconia layer of thickness d on compliant substrate: C cone crack at contact periphery, Y quasiplastic zone from yield deformation, R radial crack from intaglio surface.

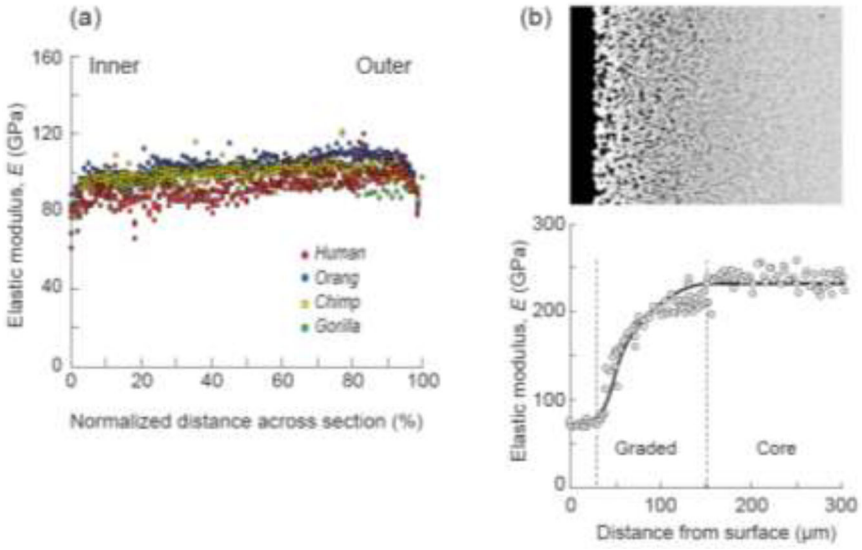

2.

Use of Berkovich nanoindentation to probe elastic modulus variations in dental structures. (a) Across longitudinal section in great ape tooth enamel, showing gradient in values between outer and inner surfaces [58]. (b) At cross section of in-house glass-infiltrated 3Y-TZP (TZ-3Y-E grade, Tosoh, Tokyo, Japan), with value close to that of dental porcelain and tooth enamel at cameo surface increasing to that of core zirconia at depth ~ 150 μm [12].

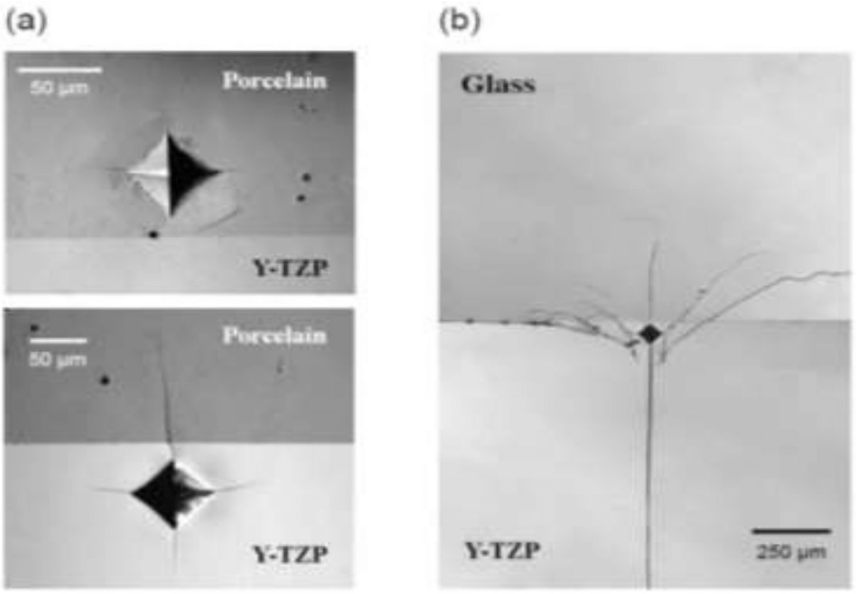

3.

Corner cracks from Vickers indentations near fused interfaces in bilayers [46]. (a) Porcelain (Lava Ceram, 3M ESPE AG, Seefeld, Germany) on 3Y-TZP (Lava Frame, 3M ESPE AG, Seefeld, Germany), CTE mismatch $< 0.5\times10^{-6}\ °C^{-1}$. Note how cracks either arrest, delaminate, or penetrate interface. (b) Borosilicate glass on same 3Y-TZP, CTE mismatch ~ $5\times10^{-6}\ °C^{-1}$. Large residual stresses in latter case have caused catastrophic failure of the bilayer.

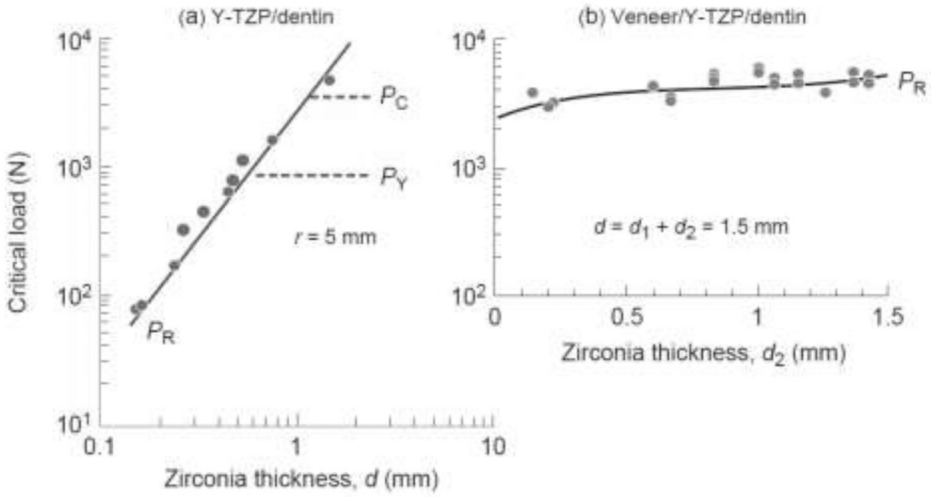

4.

Critical loads to initiate radial cracks (P_R), cone crack (P_C), and quasiplastic yield deformation (P_Y) in flat 3Y-TZP (Prozyr Y-TZP, Norton, East Granby, CT) on a compliant substrate, as function of zirconia thickness. (a) 3Y-TZP layer of variable d on substrate, P_C and P_Y computed for nominal r = 5 mm [86]. (b) Veneer layer of thickness d_1 on same 3Y-TZP core of thickness d_2, with fixed *net* thickness d = 1.5 mm [67]. P_R data from tests on polycarbonate substrates scaled for equivalent dentin substrates using eqn. 1.

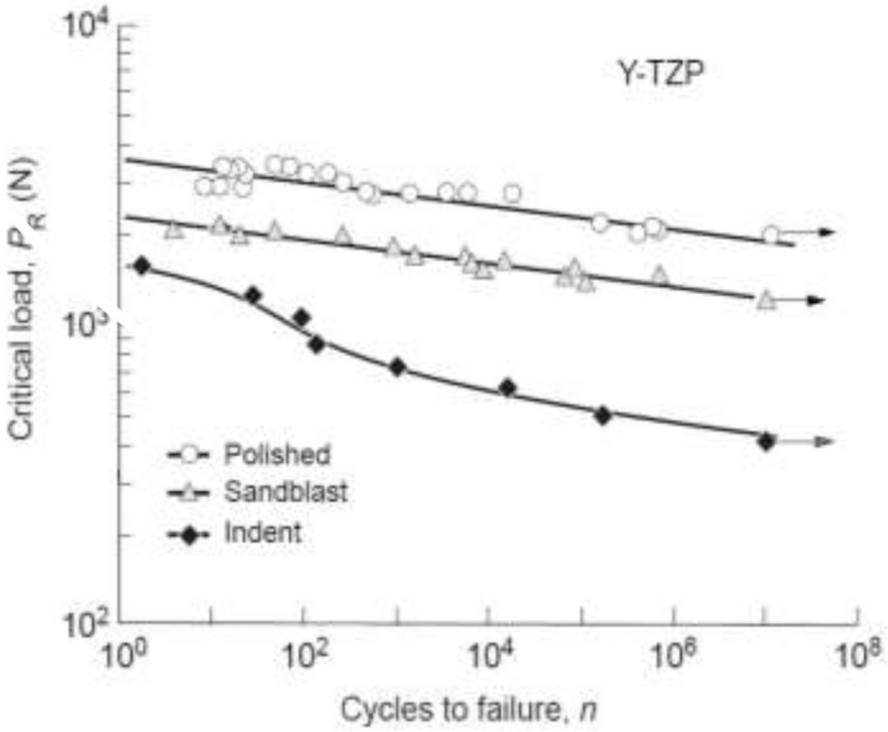

5.

Critical loads P_R for intaglio radial cracking in monolithic Y-TZP (Prozyr Y-TZP, Norton, East Granby, CT) on a dentin substrate as function of number of contacts with a hard sphere [52]. Data shown for as-polished, sandblasted, and indented (Vickers, 10 N) zirconia undersurfaces. Linear fits to polished and sandblasted cases are in accordance with strength loss from moisture-assisted slow crack growth. Curve through data for indented surfaces is empirical fit, revealing enhanced degradation from mechanical fatigue for flaws within quasiplastic contact zone. Arrows indicate 'runouts', i.e. no failure after 10^7 cycles.

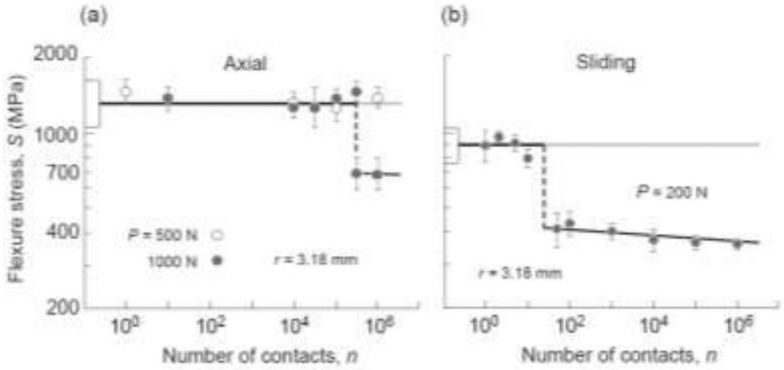

6.

Inert strength of zirconia after occlusal damage from cyclic contacts with hard sphere of radius $r = 3.18$ mm, in water. (a) Axial loading of 3Y-TZP bars (Prozyr Y-TZP, Norton, East Granby, CT) with tungsten carbide indenter at two loads shown [55]. (b) Sliding loading on 3Y-TZP discs (Zpex, Heany Dental, Scottsville, NY) with zirconia sphere in mouth-motion machine at relatively low load (data courtesy Marcia Borba and Tomoyuki Okamoto). Data points for specimens on the lower solid lines are failures are from contact sites. Boxes at left axis are strengths of unindented specimens (standard deviation bounds). Abrupt drops in strength after cycling correspond to initiation of cone or other macroscopic cracks from quasiplastic zone.